Honokiol Attenuates Lipotoxicity in Hepatocytes via Activating SIRT3-AMPK Mediated Lipophagy

Zhang Tian
University of Macau Institute of Chinese Medical Sciences https://orcid.org/0000-0002-4871-1771
Jingxin Liu
Shenzhen Technology University
Jianzhong Zhu
University of Macau
Rongsong Li
Shenzhen Technology University
Ligen Lin (ligenl@um.edu.mo)
University of Macau https://orcid.org/0000-0002-6799-5327

Research Article

Keywords: honokiol, hepatocytes, lipid accumulation, lipophagy, SIRT3, lipolysis

Posted Date: August 17th, 2021

DOI: https://doi.org/10.21203/rs.3.rs-798948/v1

Abstract

Background: Non-alcoholic fatty liver disease (NAFLD) is characterized by ectopic accumulation of triglycerides in the liver. Emerging evidence has demonstrated that lipophagy regulates lipid mobilization and energy homeostasis in liver. Sirtuin 3 (SIRT3), a mitochondrial NAD^+-dependent deacetylase, modulates the activities of several substrates involving in autophagy and energy metabolism. Honokiol (HK) is a natural lignan from the plants of *Magnolia* genus that exhibits potent liver protective property.

Methods: AML12 was challenged with 500 μM palmitic acid and 250 μM oleic acid mixture solution to induce lipotoxicity. The expression of autophagy-related and AMP-activated protein kinase (AMPK) pathway proteins was evaluated by Western blotting and immunofluorescence staining. Intracellular lipid accumulation was validated by Nile red staining. Molecular docking analysis was performed on AutoDock 4.2.

Results: HK (5 and 10 μM) was found to attenuate lipid accumulation through promoting SIRT3-AMPK-mediated autophagy, mainly on lipid droplets. HK had hydrophobic interaction with amino acid residues (PHE294, GLU323 and VAL324) and NAD^+. Moreover, HK improved mitochondrial function to enhance lipolysis, through decreasing the acetylated long-chain acyl-CoA dehydrogenase level.

Conclusions: These results suggest that HK could ameliorate lipotoxicity in hepatocytes by activating SIRT3-AMPK-lipophagy axis, which might be a potential therapeutic agent against NAFLD.

Background

Non-alcoholic fatty liver disease (NAFLD) is prevailing in recent decades, which is closely related to non-alcoholic steatohepatitis (NASH), liver fibrosis and even hepatocellular carcinoma [1]. NAFLD is resulted from the ectopic accumulation of liver lipid, accompanied by lipotoxicity and subsequent metabolic abnormalities [2]. NAFLD occurs when the abnormal accumulation of triglycerides (TG) cannot compensate by the consumption [3]. Autophagy is a cellular recycling process that achieves energy homeostasis through lysosomal dependent degradation. The development of NAFLD is positively associated with impaired autophagy [4, 5]. Lipophagy describes such a process that lipid droplets (LDs) are engulfed into autolysosomes, causing the release of free fatty acids (FFAs) [6]. This actually opens up the possibility to alleviate lipotoxicity in hepatocytes.

Sirtuin 3 (SIRT3), mainly found in mitochondria, is a nicotinamide adenine dinucleotide (NAD^+)-dependent deacetylase [7]. SIRT3 acts predominantly as a pro-survival factor to protect hepatocytes against oxidative stress [8]. We recently discovered that SIRT3-mediated autophagy promotes lipid mobilization in adipocytes via activating AMP-activated protein kinase (AMPK) [9]. Furthermore, SIRT3 activates lipophagy and chaperon-mediated autophagy to protect hepatocytes from lipotoxicity [10]. These findings imply that SIRT3 regulates lipid homeostasis and is a potential target for NAFLD. Unfortunately, the only ways to activate SIRT3 are calorie limitation and endurance training [11, 12]. The small molecular SIRT3 activators are limited. Honokiol [2-(4-hydroxy-3-prop-2-enyl-phenyl)-4-prop-2-enyl-phenol,

HK], a natural lignan ubiqutous in the *Magnolia* genus, is traditional used in Asian ethnic medicines [13, 14]. HK was demonstrated to alleviate hepatic steatosis in various models [15–18]. HK acts as an activator of SIRT3 to reverse cardiac hypertrophy and alleviate oxidative stress [19–21]. Additionally, the binding of HK and SIRT3 activates AMPK to regulate in cellular energy homeostasis [20]. These findings suggest a possible role of HK in regulating hepatic lipid homeostsis.

To validate the hypothesis that HK stimulates lipid mobilization in hepatocytes by promoting SIRT3-mediated lipophagy, we evaluated the regulative effect of HK on lipid accumulation hepatocytes with lipid challege, and explored the role of SIRT3 in HK induced lipophagy and enhaced mitochondrial function, which demonstrated HK is potrential candidate for the treatment of NAFLD.

Materials And Methods

Materials

Dulbecco's Modified Eagle Medium (DMEM), penicillin-streptomycin (P/S), fetal bovine serum (FBS), phosphate-buffered saline (PBS) and 0.25% (w/v) trypsin-EDTA were purchased from Gibco (Gaithersburg, MD, USA). ITS-G (5 mg/mL insulin, 5 mg/L transferrin, 5 μg/L selenous acid) was offered by Peiyuan Biotechnology, Shanghai, China. 3-(4,5-dimethylthiazol-2-yl)-2,5-diphenyltetrazolium bromide (MTT), HK, puromycin, oleic acid, palmitic acid, fatty acid free bovine serum albumin, isoproterenol, DAPI, Oil Red-O, and Free Glycerol Reagent were offered by Sigma–Aldrich (St. Louis, MO, USA). Lipofectamine 3000 Reagent, BCA protein assay kit, SuperSignal West Femto Maximum Sensitivity Substrate and Texas Red-conjugated secondary antibodies were bought from Thermo-Fisher (Grand Island, NY, USA). RIPA lysis buffer and ad-mCherry-GFP-LC3 (#C3011) were offered by Beyotime Biotechnology (Shanghai, China). Triton X-100 and PVDF membranes were supplied by Bio-Rad laboratories (Hercules, CA, USA). The shRNA targeting SIRT3 (mouse, sc-61556), scrambled shRNA (mouse, sc-1080600), and shRNA transfection reagent (mouse, sc-108061) were provided by Santa Cruz Biotechnology (Santa Cruz, CA, USA).

Cell culture and treatments

AML12 cells, obtained from ATCC (Rockville, MD, USA), were cultured in DMEM (supplemented with 10% FBS and ITS-G) in a humidified incubator (5% CO_2, 37 °C). Palmitic and oleic acid were prepareded with 75% (v/v) ethanol at 55 °C and were diluted to 500 μM and 250 μM with DMEM containing 1% fatty acid free bovine serum albumin (w/v), respectively. To make a mixture solution of palmtic acid and oleic acid (P/O), the two solutions were sterilized with 0.2 μm filter membrane after shaking in a incubator for 2 h.

Cell viability

The viability of AML12 cells was determined by MTT as previously described [10]. The working solution of HK was prepared immediately before use through diluting the stock solution (10 mM in DMSO) with fresh complete medium.

Immunoblotting

Protein concentration was quantified with a BCA Protein Assay Kit after lysing the cells with RIPA lysis buffer (containing 1% protease inhibitor cocktail and 1% phenylmethane sulfonylflfluoride). Proteins (20–30 μg) were separated using 5–12% SDS-PAGE and then transferred to PVDF membranes. The membranes were firstly blocked with 5% defatted milk for 2 h at room temperature, followed by overnight incubation of specific primary antibodies at 4 °C and further incubation of secondary antibodies for 1 h at room temperature. SuperSignal West Femto Maximum Sensitivity Substrate kit was used to develop the signals. Visualization of the specific protein bands were achieved on the ChemiDoc MP Imaging System, and the bands were quantitated with Image Lab 5.1 (Bio-Rad laboratories, Hercules, CA, USA).

RNA trans fection and adenovirus infection

Cells were transfected with 2 μg shRNA using Lipofectamine 3000 (Thermo-Fihser). After 6 h, cells were switched into fresh medium and incubated for a day. Then, cells were successively selected with puromycin (2 μg/mL) for 6 days and puromycin (4 μg/mL) for another 6 days before cells were pooled together.

Cells (2×10^5) were seeded in 6-well plates and infected with 10 μL Ad-mCherry-GFP-LC3 (multiplicity of infection = 5) using Lipofectamine 3000 after incubating for 24 h, followed by switch to fresh medium after 6 h and incubation for an additional 24 h. Then, cells were pooled together and ready for further investigations.

Confocal immunofluorescence microscopy

After seeding, cells were fixed in formalin (10%), blocked with goat serum (2.5%), and incubated with primary antibodies as well as Texas Red-conjugated secondary antibodies. The nuclei were stained with DAPI. Leica TCS SP8 confocal fluorescence microscope (Leica, Buffalo Grove, IL, USA) was used to capture the images.

Nile red staining

Nile red staining was conducted as previously reported [22]. Briefly, AML12 hepatocytes were fixed with formaldehyde (10%) and stained with Nile red (1 μg/mL). After incubating for 30 min at 4 °C and washing with PBS, the stained LDs were observed with fluorescence microscopy, and quantitated with flow cytometer with excitation and emission wavelength at 530 and 590 nm, respectively.

Determination of cellular triglycerides

TG content in cell lysate was determined by using commercial kits (Nanjing Jiancheng Bioengineering Institute, Nanjing, Jiangsu, China) and normalized by protein concentration.

Molecular docking analysis

Docking was performed on *AutoDock 4.2*. The crystal structure of the quaternary complex (SIRT3, a substrate, NAD^+, and the specific agonist amiodarone hydrochloride; PDB ID: 5H4D) [23] was employed as the receptor. The protein was firstly prepared at pH 7.4 with all the water molecules removed and corresponding hydrogen atoms added. The 3D structure of HK was downloaded from the *PubChem* database. Gasteiger charge was calculated and AD4 atom type was assigned, and a 50 Å × 48 Å × 40 Å grid box with 375 Å spacing was placed to include the surface of the catalytic cleft with the assistance of amiodarone hydrochloride. The genetic searching algorithm was chosen for docking calculations, and 50 genetic algorithm runs were performed. Other parameters were set as default. The acquired poses were clustered with a tolerance of 2.0 Å.

Lipid droplets isolation

LDs were isolated from AML12 hepatocytes as described previously [10]. Briefly, AML12 cells were lysed in hypotonic buffer (50 mM HEPES, 1 mM EDTA and 2 mM $MgCl_2$, pH 7.4) supplemented with protease inhibitors after scaping and homogenized with 50 strokes in a Dounce homogenizer. After spinning down at 1500 g for 5 min, post-nuclear fractions were mixed with equal volumes of 1.05 M sucrose in isotonic buffer (50 mM HEPES, 100 mM KCl, 2 mM $MgCl_2$) and centrifuged at 100,000 *g* for 2 h to remove Golgi, rough endoplasmic reticulum, mitochondria, and peroxisomes. The acquired supernatant was adjusted to 1 M sucrose in hypotonic buffer and layered on a sucrose gradient (1 mL of 0.75, 0.5, 0.25, 0.125, and 0 M sucrose solution, respectively). The sucrose gradient tube was centrifuged at 100,000 *g* for 4 h at 4 °C afterwards, followed by collection of LD fractions from the top which were delipidated with acetone and washed with acetone/ether (1:1, v:v). The pellet was dried under nitrogen and resuspended in protein lysis buffer. The protein concentration of LD fractions was analysed by BCA Protein Assay kit, and subsequent western blotting was performed.

Cellular thermal shift assay (CETSA)

Cells were lysed after pretreatment with or without HK (10 μM) for 12 h. The lysates were centrifuged at 12,000 *g* for 10 min at 4 °C after incubating in ice for 10 min. The protein concentration was determined and adjusted to 3 μg/μL using RIPA lysis buffer. Cell lysates (50 μL) were transferred to new tubes and heated for 3 min at various temperature (50–90°C) on a thermal cycler. After standing in ice for 10 min, soluble proteins were obtained by centrifugation at 12,000 *g* for 20 min at 4 °C and analyzed by western blotting [24].

Mitochondrial membrane potential assay

The fluorescent dye Rhodamine123 was employed to detect the mitochondrial membrane potential. Specifically, AML12 cells were cultured in the presence or absence of HK, and stained with Rhodamine123 (10 μM) for 10 min. Then, cells were washed twice with PBS, trypsinized and collected into a 1.5 mL tube. The change of membrane potential was qualitatively observed on an In Cell Analyzer 2000 (GE Healthcare Life Sciences, Chicago, IL, USA).

Intracellular reactive oxygen species (ROS) detection

Intracellular ROS levels were detected using DCFH-DA as previously described [25]. Briefly, cells (1×10^5) were seeded into 96-well black multitier plate (clear bottom) and then cultured overnight. The cells were treated with or without HK. After 12 h, the cells were incubated with DCFH-DA (10 μM) at 37 °C in the dark for 15 min. Fluorescence intensity was analyzed through FACSCalibur flow cytometry (BD, Lake Franklin, NJ, USA).

Isoproterenol-stimulated lipolysis

The lipolysis activity of AML12 cells was measured as described previously [26]. Cells were incubated with 10 μM isoproterenol (stimulated condition) or DMSO (basal condition) for 2 h. Subsequently, the medium was collected and heated at 85 °C for 10 min. Clear supernatant (10 μL), acquired through centrifugation, was used to determine the free glycerol content using Free Glycerol Reagent. Lipolysis activity was represented by glycerol concentrations and normalized by protein concentration.

Immunoprecipitation

Immunoprecipitation was performed as described previously [27]. Briefly, cell lysates (3 mg protein) were mixed with the indicated antibody (2 μg) at 4 °C overnight. Then protein A/G-agarose beads (20 μL) were added to the mixture, which was incubated on a rotator for 4 h at 4 °C. Immune complexes were washed twice with lysis buffer supplemented with complete mini-protease inhibitor cocktail after washing the beads for three times with PBS. Bound proteins were boiled in sample preparation buffer for 5 min and then immunoblotting was conducted.

Statistical analysis

All experimental data were expressed as mean ± S.D., and sample size for each experiment corresponds to three biological replicates. Data analysis was finished on GraphPad Prism-6 (GraphPad Software, San Diego, CA, USA), where significant differences between groups were evaluated by one-way analysis of variance (ANOVA) followed by Dunnet's multiple comparisons test ($p < 0.05$ was considered as significant differences). Where statistical significance is evaluated, variance between groups is confirmed to be similar between comparison groups (control vs. experimental) and the statistical analysis is considered appropriate.

Results

Honokiol attenuates lipid accumulation in lipotoxic hepatocytes through promoting autophagy

P/O (palmitic acid and oleic acid mixture) is widely used to induce lipotoxicity *in vitro* baecause of its same effect in inducing steatosis and lower cytotoxicity than palmitic acid alone [28, 29]. Herein, lipid accumulation in AML12 cells was realized by inducement with P/O (the ratio of oleic acid to palmitic acid is 1:2). Firstly, we evaluated the effects of HK against P/O-induced lipid accumulation in AML12 cells. HK

did not exhibit obvious cytotoxicity on AML12 cells up to 10 μM [21]. Interestingly, a 2.7-fold increase of lipid content was observed after P/O stimulation, and HK attenuated this effect dose-dependently, which was comparable with the positive control resveratrol, as indicated by Nile red staining and its quantitative analyses (Fig. 1A, 1B). P/O-induced increase of TGs in AML12 cells was also reversed by HK treatment (Fig. 1C).

Impaired autophagy results in increased lipid storage in hepatocytes [30]. As shown in Fig. 1D, after P/O-treatment, there is a shrinkage in Beclin1 level and the ratio of LC3-II/LC3-I to approximately 48–75%, whereas p62 level was elevated to 267%, compared with those of the control cells, suggesting impaired autophagy in AML12 cells. Intriguingly, HK treatment reversed the above changes in dose-dependent manners (Fig. 1D). Meanwhile, HK also enhanced autophagy in unstimulated AML12 cells (Fig. 1D). To see whether HK enhanced autophagic flux, we infected the AML12 cells with mRFP-GFP-LC3 adenovirus to label autophagosomal formation. As shown in Fig. 1E and 1F, impaired autophagy was reflected by the decreased both red and green puncta after P/O treatment. More mRFP-LC3 puncta were observed in HK-treated cells as expected, suggesting that autophagic flux was improved with undisturbed lysosomal function and/or autophagosome-lysosome fusion. Furthermore, the fluorescent images indicated that autophagosome formation, which was largely co-localized with LDs (Fig. 1G), was anhanced with HK. These results indicated that HK mitigates lipid accumulation in lipotoxic hepatocytes through promoting autophagy.

Honokiol attenuates lipid accumulation through SIRT3-mediated autophagy

SIRT3 overexpression protects hepatocytes from lipotoxicity though promoting lipophagy and chaperon-mediated autophagy to [10]. Interestingly, HK treatment dose-dependently increased SIRT3 level in P/O-treated AML12 cells (Fig. 2A). To experimentally verify the interaction between HK and SIRT3 deacetylase, CETSA was performed on AML12 cells treated with or without HK. Compared to the control cells, the thermal stability of SIRT3 was strongly enhanced by HK at various temperatures (Fig. 2B). To verify the interaction pattern between HK and SIRT3, docking analysis was conducted. Clustering analysis showed the predominant cluster had the lowest binding energy with the best pose owing a − 7.2 kcal/mol (Fig. 2C). HK had hydrophobic interaction with amino acid residues (PHE294, GLU323 and VAL324) and NAD^+ (Fig. 2D). Additionally, it was hydrogen bonded with an oxygen on the NAD^+ (Fig. 2D).

To evaluate the role of HK-driven SIRT3 in reducing lipid accumulation in hepatocytes, thr SIRT3 knocking down AML12 cell line (SIRT3KD) was generated using shRNA targeting SIRT3. As expected, SIRT3 silencing partially blocked the lipid lowering effects of HK in P/O-stimulated AML12 cells (Fig. 2E). HK treatment increased the expression of LC3II, and reduced lipid content and LD size in P/O-treated AML12 cells; whereas, silencing of SIRT3 almost abrogated the effects of HK (Fig. 2F).

Next, we determined whether HK treatment is sufficient for inducing lipophagy and the pharmacological activation of SIRT3 plays a role in this process. The LD fraction was isolated from scrambled and SIRT3KD AML12 cells treated with or without HK, and enrichment of LC3-II, Beclin1 and decreased p62 were observed in LDs, but not in homogenates after treatment of HK; and deletion of SIRT3 almost

reversed HK-driven activation of autophagy in isolated LDs (Fig. 2G). These observations indicated HK treatment induced lipophagy rather than bulky autophagy to alleviate lipid accumulation and SIRT3 is required in HK-induced lipophagy.

Honokiol alleviates lipid accumulation through SIRT3-AMPK-induced autophagy

SIRT3 activates autophagy through the AMP-activated kinase (AMPK) pathway in palmitate-stressed hepatocytes [10]. To elucidate the mechanism of HK on SIRT3-mediated autophagy, the phosphorylation level of AMPK was determined in HK treated hepatocytes. The HK dose-dependently increased the phosphorylated AMPK in P/O treated AML12 cells as expected (Fig. 3A). Compound C (CC), an inhibitor to AMPK, remarkably diminished the effect of HK on activating autophagy (Fig. 3B). As shown in Fig. 3C and 3D, treatment of CC reversed the reducing effect of HK on lipid and TG content, supporting that HK alleviated lipid accumulation in AML12 cells via activating AMPK signaling pathway. These results suggested that the effect of HK on lowering lipid accumulation was mediated through SIRT3-AMPK-mediated autophagy.

Honokiol attenuates lipid accumulation by restoring mitochondrial function

Next, we assumed the lipid lowering effect of HK was involved in enhanced mitochondrial function. Therefore, we determined the mitochondrial membrane potential by using Rhodamine 123 staining. The results showed P/O stimulation disrupted mitochondrial membrane potential, whereas HK-treated cells exhibited higher mitochondrial membrane potential, suggesting improved mitochondrial function (Fig. 4A). Meanwhile, lipid challenge lead to high level of intracellular ROS and reduced mitochondrial. HK treatment alleviated oxidative stress and slightly enhanced mitochondrial biogenesis in P/O-treated AML12 cells (Fig. 4B and 4C). Activation of autophagy not only shifts lipids to the lysosome for degradation by acid lipases, but enhances lipolysis by neutral lipases [10]. HK enhanced lipolysis in a dose-dependent manner in isoproterenol-stimulated cells, but not the control cells (Fig. 4D). Long-chain acyl-CoA dehydrogenase (LCAD) is a deacetylating substrate of SIRT3 [31]. HK decreased the acetylated LCAD level in a dose-dependently, but did not change the total LCAD level (Fig. 4E). Taken together, HK rescues hepatocytes from P/O-induced lipid accumulation by maintaining mitochondrial function and promoting lipolysis.

Discussion

Increasing evidence has uncovered a positive connection between lipophagy and the onset of NAFLD. Organisms regulate FFAs release to supply metabolic demand by lipophagy [32]. Impaired autophagy leads to excessive lipid accumulation in liver to cause hepatic steatosis [33, 34]. HK has been found to activate autophagy in several cancer cells [35–37]. Herein, we found HK attenuates lipid accumulation in lipotoxic hepatocytes through promoting SIRT3-AMPK-induced autophagy and mitochondrial function. To fully verify the role of HK in treating NAFLD, diet-induced fatty liver mice model and/or genetically obese mice model should be recruited in the future.

Autophagy accounts for a major part of lipolysis in liver. Consequently, autophagy blockage through knockdown of the key autophagic genes like Atgs in hepatocytes, led to an increase of LDs in cells even under normal nutritional conditions [38]. Interestingly, impaired autophagy further deteriorated LDs accumulation, leading to hepatotoxicity and severe steatosis [39]. In our current study, HK was found to activate lipophagy, stimulate lipolysis under isoproterenol treated condition and decrease the acetylated LCAD level. These results indicated that HK protects hepatocytes against lipotoxicity through enhancing lipophagy and lipolysis.

Liver contains a large number of mitochondria, which are the predominant source of intracellular ROS. Excessive ROS accumulation results in cell death through the oxidation of polyunsaturated fatty acids [40]. Mitochondrial homeostasis was interrupted when the hepatocytes were exposed to P/O stimulation, accompanied with decreased mitochondrial content and increased ROS production. Interestingly, high dose of HK maintained mitochondrial integrity in hepatocytes under lipotoxic stress. In fact, mitochondrial biogenesis acts as a critical factor for mitochondrial quantity, and HK was found to facilitate the process by targeting PGC-1α [41]. Herein, HK did not affect mitochondrial biogenesis, but enhanced mitochondrial function in lipotoxic hepatocytes. SIRT3 may also be involved in mitochondrial renewal and hepatocyte proliferation through mitophagy mechanisms [42]. Future studies are required to fully elucidate how HK regulates mitophagy in the context of hepatocellular lipotoxicity.

AMPK directly stimulates mitochondrial energy production and strengthens mitochondrial biogenesis [43]. The current data showed that HK promoted the phosphorylation of AMPK, which could directly activate autophagy. Inhibition of AMPK reversed the lipid lowering effect of HK. In general, HK activates autophagy and attenuates lipid accumulation in P/O-treated hepatocytes through activating AMPK.

The most widespread and prevailing model describing the development of NAFLD is the “multiple-hit hypothesis”, where the “first hit”, hepatic lipid accumulation, induces lipotoxicity or steatosis, rendering liver more vulnerable to “subsequent hits” injury, such as mitochondrial dysfunction and oxidative stress, which in turn leads to steatohepatitis and cirrhosis, and eventually hepatocellular carcinoma [44]. In the previous study, we reported that HK scavenges excessive ROS and repairs cellular damages in oxidative injured hepatocytes. Herein, we further found that HK activates lipophagy to promote LD breakdown, leading to reduced lipotoxicity in hepatocytes. Taken together, HK might protect hepatocytes against oxidative stress and alleviate lipotoxicity, rendering it a potential candidate to treat NAFLD against multiple hits.

Conclusions

In conclusion, we verified HK protects hepatocytes against lipotoxic stress through enhancing SIRT3-AMPK-induced lipophagy, and maintain mitochondrial morphology and integrity (Fig. 5). HK could be a potential candidate in the treatment of NAFLD.

Abbreviations

AMPK, AMP-activated protein kinase; CC, Compound C; CETSA, cellular thermal shift assay; FFAs, free fatty acids; HCC, hepatocellular carcinoma; HFD, high-fat diet; HK, honokiol; LCAD, long-chain acyl-CoA dehydrogenase; LD, lipid droplet; 3-MA, 3-methyladenine; NASH, non-alcoholic steatohepatitis; NAFLD, non-alcoholic fatty liver disease; P/O, palmitic acid/oleic acid; ROS, reactive oxygen species; SIRT3, Sirtuin 3; TG, triglyceride.

Declarations

Acknowledgements

The authors thank the technical team of Institute of Chinse Medical Sciences in University of Macau for their valuable assistance.

Authors' contributions

Tian Zhang: Conceptualization, Investigation, Writing original draft. Jingxiu Liu: Conceptualization, Investigation, Review & editing. Jianzhong Zhu: Investigation, Review & editing. Rongsong Li: Resources, Review & editing. Ligen Lin: Conceptualization, Methodology, Validation, Writing review & editing, Supervision.

Funding

Financial support by the Science and Technology Development Fund, Macao SAR (File no. FDCT 0031/2019/A1), the Research Fund of University of Macau (MYRG2017-00109-ICMS and MYRG2018-00037-ICMS), and National Natural Science Foundation of China (81872754) are gratefully acknowledged.

Availability of data and materials

Not applicable.

Ethics approval and consent to participate

Not applicable.

Consent for publication

Not applicable.

Competing interests

The authors declare that they have no competing interests.

References

1. Lu FB, Zheng KI, Rios RS, Targher G, Byrne CD, Zheng MH. Global epidemiology of lean non-alcoholic fatty liver disease: A systematic review and meta-analysis. J Gastroenterol Hepatol. 2020;35(12):2041–50.
2. Cohen JC, Horton JD, Hobbs HH. Human fatty liver disease: old questions and new insights. Science. 2011;332(6037):1519–23.
3. Han YM, Hu ZM, Cui AY, Liu ZS, Ma FG, Xue YQ, et al. Post-translational regulation of lipogenesis via AMPK-dependent phosphorylation of insulin-induced gene. Nat Commun. 2019;10:623.
4. Gonzalez-Rodriguez A, Mayoral R, Agra N, Valdecantos M P, Pardo V, Miquilena-Colina ME, et al. Impaired autophagic flux is associated with increased endoplasmic reticulum stress during the development of NAFLD. Cell Death Dis. 2014;5:e1179.
5. Baerga R, Zhang Y, Chen P H, Goldman S, Jin S. Targeted deletion of autophagy-related 5 (atg5) impairs adipogenesis in a cellular model and in mice. Autophagy. 2009;5(8):1118–30.
6. Singh R, Kaushik S, Wang Y, Xiang Y, Novak I, Komatsu M, et al. Autophagy regulates lipid metabolism. Nature. 2009;458(7242):1131–5.
7. Hirschey MD, Shimazu T, Goetzman E, Jing E, Schwer B, Lombard DB, et al. SIRT3 regulates mitochondrial fatty-acid oxidation by reversible enzyme deacetylation. Nature. 2010;464(7285):121–5.
8. Ma C, Sun Y, Pi C, Wang H, Sun H, Yu X, et al. Sirt3 attenuates oxidative stress damage and rescues cellular senescence in rat bone marrow mesenchymal stem cells by targeting superoxide dismutase 2. Front Cell Dev Biol. 2020;8:599376.
9. Zhang T, Liu J, Tong Q, Lin L. SIRT3 acts as a positive autophagy regulator to promote lipid mobilization in adipocytes via activating AMPK. Int J Mol Sci. 2020;21(2):372.
10. Zhang T, Liu J, Shen S, Tong Q, Ma X, Lin L. SIRT3 promotes lipophagy and chaperon-mediated autophagy to protect hepatocytes against lipotoxicity. Cell Death Differ. 2020;27(1):329–44.
11. Qiu X, Brown K, Hirschey MD, Verdin E, Chen D. Calorie restriction reduces oxidative stress by SIRT3-mediated SOD2 activation. Cell Metab. 2010;12(6):662–7.
12. Vassilopoulos A, Pennington JD, Andresson T, Rees DM, Bosley AD, Fearnley IM, et al. SIRT3 deacetylates ATP synthase F1 complex proteins in response to nutrient- and exercise-induced stress. Antioxid Redox Signal. 2014;21(4):551–64.
13. Chou PY, Chang WC, Liu FC, Lan SJ, Sheu MJ, Chen JS. Honokiol, an active compound of Magnolia officinalis, is involved in restoring normal baroreflex sensitivity in hypercholesterolemic rabbits. Food Sci Nutr. 2020;8(2):1093–103.
14. Chen C, Zhang QW, Ye Y, Lin LG. Honokiol: A naturally occurring lignan with pleiotropic bioactivities. Chin J Nat Med. 2021;19(7):481–90.
15. Yin HQ, Kim YC, Chung YS, Kim YC, Shin YK, Lee BH. Honokiol reverses alcoholic fatty liver by inhibiting the maturation of sterol regulatory element binding protein-1c and the expression of its downstream lipogenesis genes. Toxicol Appl Pharmacol. 2009;236(1):124–30.

16. Jeong YH, Hur HJ, Jeon EJ, Park SJ, Hwang JT, Lee AS, et al. Honokiol improves liver steatosis in ovariectomized mice. Molecules. 2018;23(1):194.
17. Zhai T, Xu W, Liu Y, Qian K, Xiong Y, Chen Y. Honokiol alleviates methionine-choline deficient diet-induced hepatic steatosis and oxidative stress in C57BL/6 mice by regulating CFLAR-JNK pathway. Oxid Med Cell Longev. 2020;2020:2313641.
18. Seo MS, Kim JH, Kim HJ, Chang KC, Park SW. Honokiol activates the LKB1-AMPK signaling pathway and attenuates the lipid accumulation in hepatocytes. Toxicol Appl Pharmacol. 2015;284(2):113–24.
19. Pillai VB, Samant S, Sundaresan NR, Raghuraman H, Kim G, Bonner MY, et al. Honokiol blocks and reverses cardiac hypertrophy in mice by activating mitochondrial Sirt3. Nat Commun. 2015;6:6656.
20. Caballero EP, Mariz-Ponte N, Rigazio CS, Santamaria MH, Corral RS. Honokiol attenuates oxidative stress-dependent heart dysfunction in chronic Chagas disease by targeting AMPK / NFE2L2 / SIRT3 signaling pathway. Free Radic Biol Med; 2020;156:113–24.
21. Liu JX, Shen SN, Tong Q, Wang YT, Lin LG. Honokiol protects hepatocytes from oxidative injury through mitochondrial deacetylase SIRT3. Eur J Pharmacol. 2018;834:176–87.
22. Shen S, Liao Q, Zhang T, Pan R, Lin L. Myricanol modulates skeletal muscle-adipose tissue crosstalk to alleviate high-fat diet-induced obesity and insulin resistance. Br J Pharmacol. 2019;176(20):3983–4001.
23. Zhang S, Fu L, Liu J, Liu B. Crystal structure of hSIRT3 in complex with a specic agonist Amiodarone hydrochloride. http://doi: 10.2210/pdb5H4D/pdb.
24. Jafari R, Almqvist H, Axelsson H, Ignatushchenko M, Lundback T, Nordlund P, et al. The cellular thermal shift assay for evaluating drug target interactions in cells. Nat Protoc. 2014;9(9):2100–22.
25. Liu JX, Li D, Zhang T, Tong Q, Ye RD, Lin L G. SIRT3 protects hepatocytes from oxidative injury by enhancing ROS scavenging and mitochondrial integrity. Cell Death Dis. 2017;8:e3158.
26. Lin LG, Lee JH, Bongmba OYN, Ma XJ, Zhu XW, Sheikh-Hamad D, et al. The suppression of ghrelin signaling mitigates age-associated thermogenic impairment. Aging. 2014;6(12):1019–32.
27. Li D, Liu QY, Sun W, Chen XP, Wang Y, Sun YX, et al. 1,3,6,7-Tetrahydroxy-8-prenylxanthone ameliorates inflammatory responses resulting from the paracrine interaction of adipocytes and macrophages. Br J Pharmacol. 2018;175(10):1590–606.
28. Ricchi M, Odoardi MR, Carulli L, Anzivino C, Ballestri S, Pinetti A, et al. Differential effect of oleic and palmitic acid on lipid accumulation and apoptosis in cultured hepatocytes. J Gastroenterol Hepatol. 2009;24(5):830–40.
29. Moravcova A, Cervinkova Z, Kucera O, Mezera V, Rychtrmoc D, Lotkova H. The effect of oleic and palmitic acid on induction of steatosis and cytotoxicity on rat hepatocytes in primary culture. Physiol Res. 2015;64(Suppl 5):S627–36.
30. Zhang Y, Goldman S, Baerga R, Zhao Y, Komatsu M, Jin S. Adipose-specific deletion of autophagy-related gene 7 (atg7) in mice reveals a role in adipogenesis. Proc Natl Acad Sci USA. 2009;106(47):19860–5.

31. Tseng AH, Shieh SS, Wang DL. SIRT3 deacetylates FOXO3 to protect mitochondria against oxidative damage. Free Radic Biol Med. 2013;63:222–34.
32. Rambold AS, Cohen S, Lippincott-Schwartz J. Fatty acid trafficking in starved cells: regulation by lipid droplet lipolysis, autophagy, and mitochondrial fusion dynamics. Dev Cell. 2015;32(6):678–92.
33. Yang L, Li P, Fu S, Calay ES, Hotamisligil GS. Defective hepatic autophagy in obesity promotes ER stress and causes insulin resistance. Cell Metab. 2010;11(6):467–78.
34. Sarkar S, Perlstein EO, Imarisio S, Pineau S, Cordenier A, Maglathlin R L, et al. Small molecules enhance autophagy and reduce toxicity in Huntington's disease models. Nat Chem Biol. 2007;3(6):331–8.
35. Lin MC, Lee YW, Tseng YY, Lin YW, Chen JT, Liu SH, et al. Honokiol induces autophagic apoptosis in neuroblastoma cells through a P53-dependent pathway. Am J Chin Med. 2019;47(4):895–912.
36. Li Z, Dong H, Li M, Wu Y, Liu Y, Zhao Y, et al. Honokiol induces autophagy and apoptosis of osteosarcoma through PI3K/Akt/mTOR signaling pathway. Mol Med Rep. 2018;17(2):2719–23.
37. Huang K, Chen Y, Zhang R, Wu Y, Ma Y, Fang X, et al. Honokiol induces apoptosis and autophagy via the ROS/ERK1/2 signaling pathway in human osteosarcoma cells in vitro and in vivo. Cell Death Dis. 2018;9(2):157.
38. Zechner R, Madeo F, Kratky D. Cytosolic lipolysis and lipophagy: two sides of the same coin. Nat Rev Mol Cell Biol. 2017;18(11):671–84.
39. Schulze RJ, Sathyanarayan A, Mashek DG. Breaking fat: The regulation and mechanisms of lipophagy. Biochim Biophys Acta Mol Cell Biol Lipids. 2017;1862(10 Pt B):1178–87.
40. Jaeschke H, Ramachandran A. Reactive oxygen species in the normal and acutely injured liver. J Hepatol. 2011;55(1):227–8.
41. Brenmoehl J, Hoeflich A. Dual control of mitochondrial biogenesis by sirtuin 1 and sirtuin 3. Mitochondrion. 2013;13(6):755–61.
42. Li R, Xin T, Li D, Wang C, Zhu H, Zhou H. Therapeutic effect of Sirtuin 3 on ameliorating nonalcoholic fatty liver disease: The role of the ERK-CREB pathway and Bnip3-mediated mitophagy. Redox Biol. 2018;18:229–43.
43. Wan Z, Root-McCaig J, Castellani L, Kemp BE, Steinberg GR, Wright DC. Evidence for the role of AMPK in regulating PGC-1 alpha expression and mitochondrial proteins in mouse epididymal adipose tissue. Obesity. 2014;22(3):730–8.
44. Buzzetti E, Pinzani M, Tsochatzis EA. The multiple-hit pathogenesis of non-alcoholic fatty liver disease (NAFLD). Metabolism. 2016;65(8):1038–48.

Figures

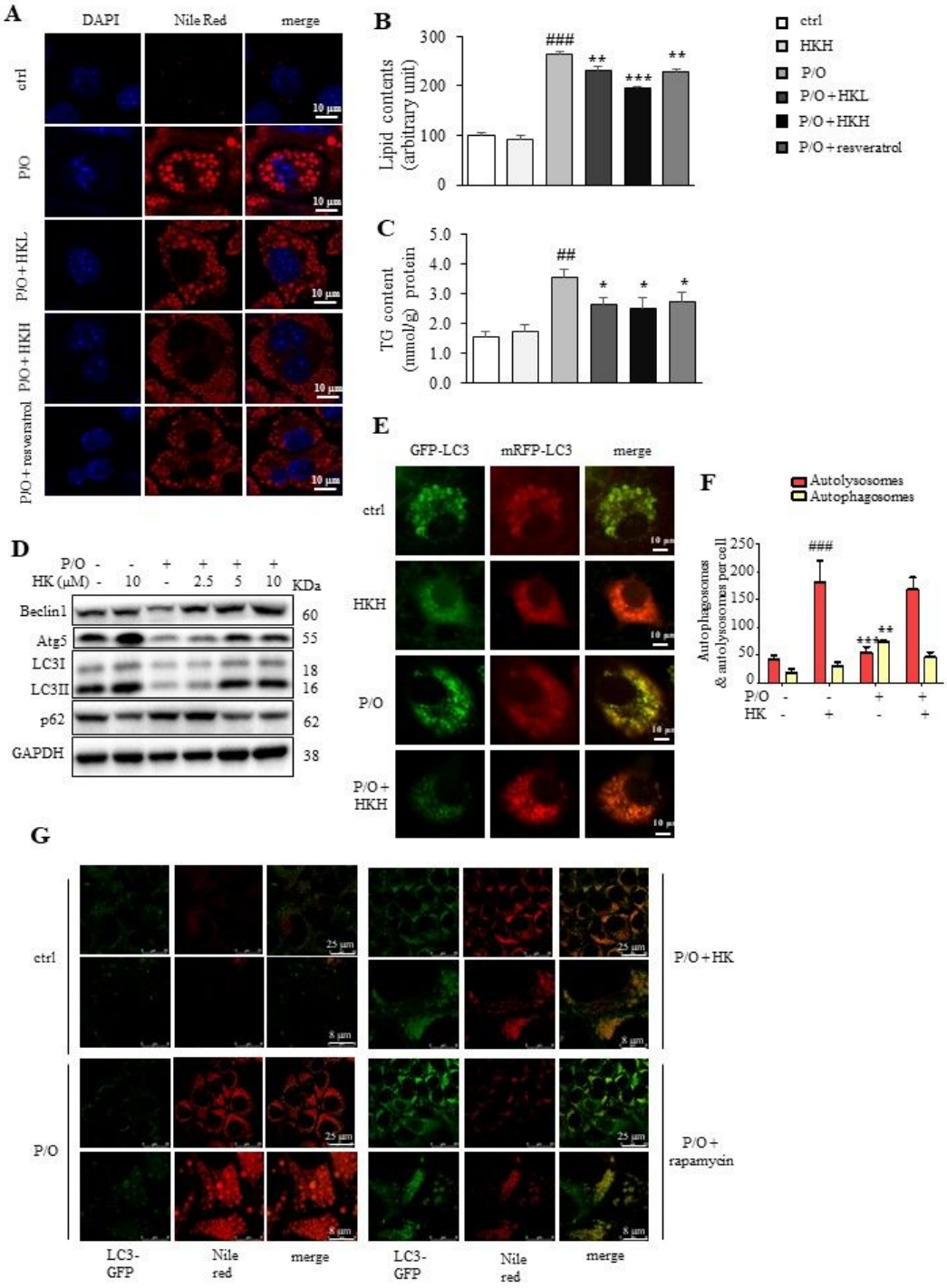

Figure 1

HK attenuates lipid accumulation in lipotoxic hepatocytes through promoting autophagy. (A) Intracellular lipid content visualized with nile red (red) staining. Nuclei were stained with DAPI (blue). Scale bar = 10 μm. Resveratrol (10 μM) was used as a positive control. (B) The lipid content determined by Nile red staining. (C) The cellular TG content. (D) Atg5, Beclin1, LC3 and p62 protein levels in P/O-stimulated AML12 hepatocytes treated without or with various concentrations of HK for 24 h. GAPDH was used as a

loading control. (E) AML12 cells were infected with the Ad-mCheryy-GFP-LC3, and treated with or without HK. The mRFP-LC3 and GFP-LC3 puncta were visualized on a confocal microscope. Scale bar = 10 μm. (F) The numbers of autophagosomes (yellow puncta) and autolysosomes (red puncta) were quantitated. (G) In P/O-stimulated AML12 hepatocytes, HK treatment induced more LC3-positive puncta (green) on LDs that were visualized with Nile red staining (red). Scale bar = 25 μm. Rapamycin was used as a positive control. Data represented means ± SD. n = 6. *p < 0.05, **p < 0.01 and ***p < 0.001, HK or resveratrol vs. P/O treatment. ##p < 0.01, ###p < 0.001, ctrl vs. P/O treatment. One-way ANOVA was used to calculate the p-values.

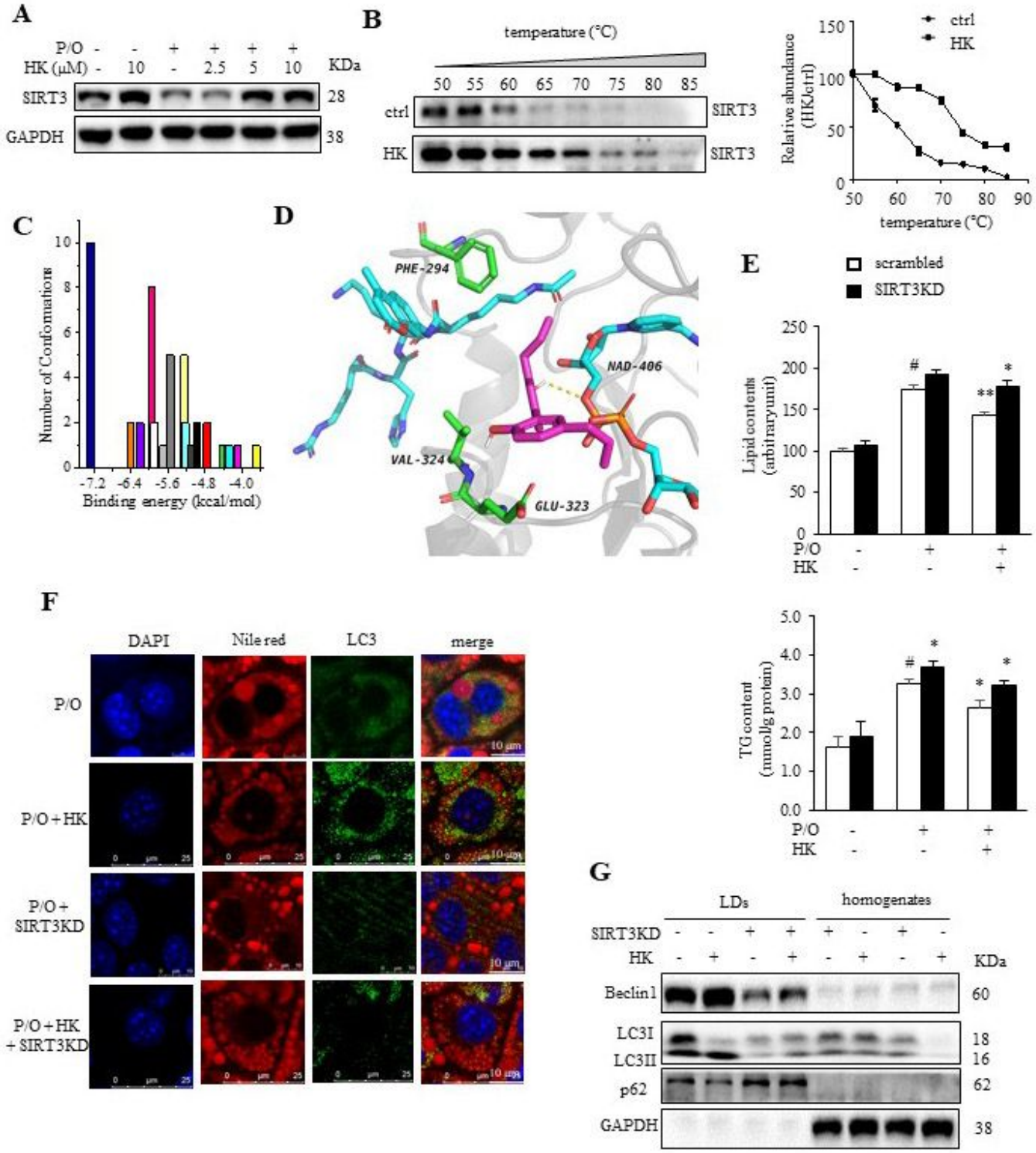

Figure 2

HK attenuates lipid accumulation through SIRT3-mediated autophagy. P/O-stimulated AML12 cells were treated without or with various concentrations of HK for 24 h. (A) SIRT3 protein levels were evaluated. GAPDH was used as a loading control. (B) CETSA was performed on AML12 cells treated with or without HK (10 μM) for 12 h. The SIRT3 protein levels were detected by using Western blotting. Data were normalized to the mean value of the respective group at 50 °C (n = 5). (C) Docking analysis of the binding

between HK and SIRT3 (PDB ID: 5H4D). Cluster analysis of the docked conformations of HK. A tolerance of 2.0 Å was used. (D) Interactions between HK and residues on SIRT3. The protein was shown in NewCartoon, and small molecules in sticks; the substrate (or NAD+), residues, and HK were colored in cyan, green, and magenta, respectively. (E) The scrambled and SIRT3KD cells were treated with or without HK for 24 h. The lipid content was determined by flow cytometry after nile red staining and the cellular TG content were determined by commercial kit. (F) SIRT3 silencing blocked HK treatment-induced co-localization of LC3 puncta (green) on LDs. LDs were visualized with nile red fluorescence. Scale bar = 25 μm. (G) HK treatment activated autophagy mainly on LDs. Data was represented as means ± SD. *p < 0.05 and **p < 0.01, HK vs. P/O treatment. #p < 0.05, ctrl vs. P/O treatment. One-way ANOVA was used to calculate the p-values.

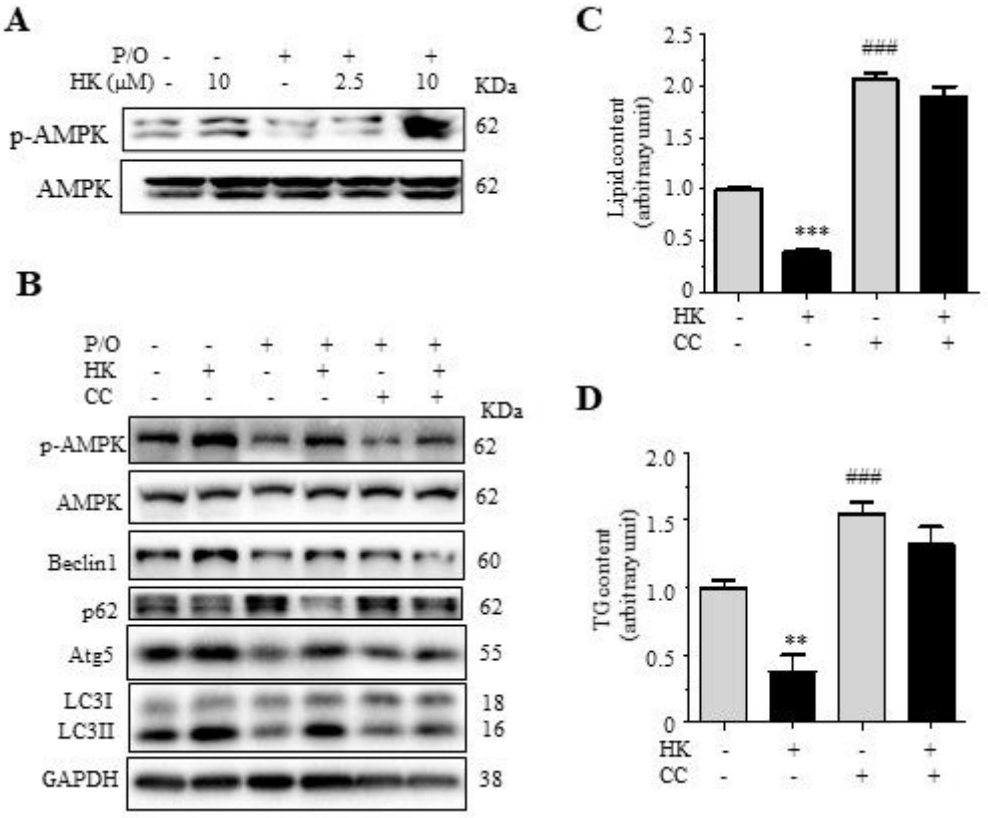

Figure 3

HK alleviates lipid accumulation through SIRT3-AMPK-induced autophagy. P/O-stimulated AML12 cells were treated without or with various concentrations of HK for 24 h. (A) p-AMPK and AMPK protein levels evaluated by Western blotting. GAPDH was used as a loading control. (B) P/O-stimulated AML12 cells were treated without or with HK (10 μM) and CC (10 μM) for 24 h. p-AMPK, AMPK, Beclin1, Atg5, p62 and LC3 protein levels were detected by Western blotting. GAPDH was used as a loading control. (C) The lipid content determined by Nile red staining. (D) The cellular TG content. Data represented means ± SD. **p < 0.01 and ***p < 0.001, HK vs. P/O treatment. ##p < 0.001, CC vs. P/O treatment. One-way ANOVA was used to calculate the p-values.

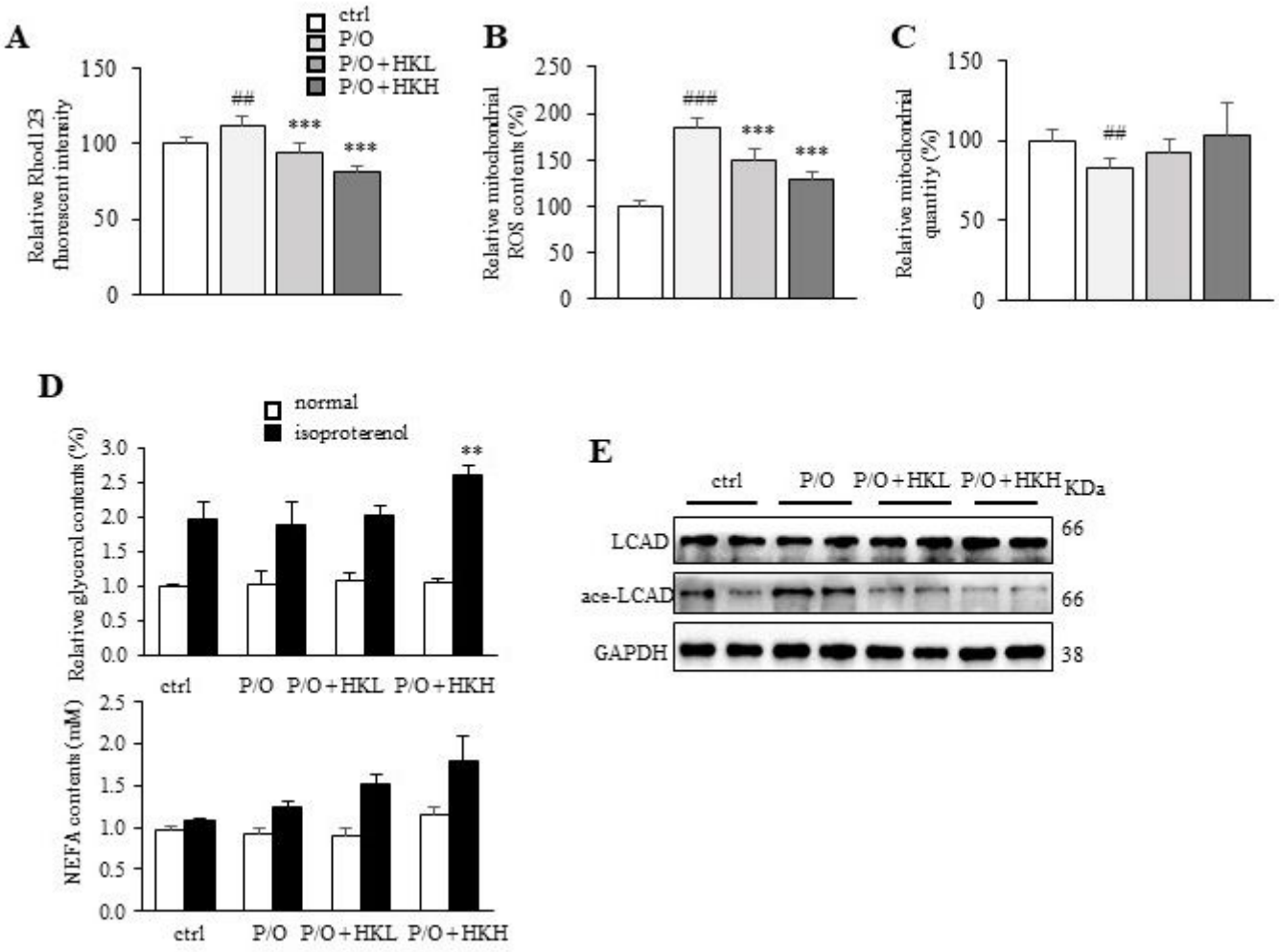

Figure 4

HK attenuates lipid accumulation by restoring mitochondrial function. AML12 cells were treated with or without HK in the presence of P/O for 24 h. (A) The relative Rhod123 fluorescent intensity. (B) Intracellular ROS accumulation levels were determined by DCFH-DA assay. (C) Mitochondria were stained by Mitochondria-green and quantitated by flow cytometry. (D) Relative glycerol content in P/O-stimulated AML12 hepatocytes under both normal and isoproterenol-induced conditions. (E) The acetylated and total LCAD levels. Data was expressed as means ± SD. **p < 0.01 and ***p < 0.001, HK vs. P/O treatment. ##p < 0.01 and ###p < 0.001 ctrl vs. P/O treatment. One-way ANOVA was used to calculate the p-values.

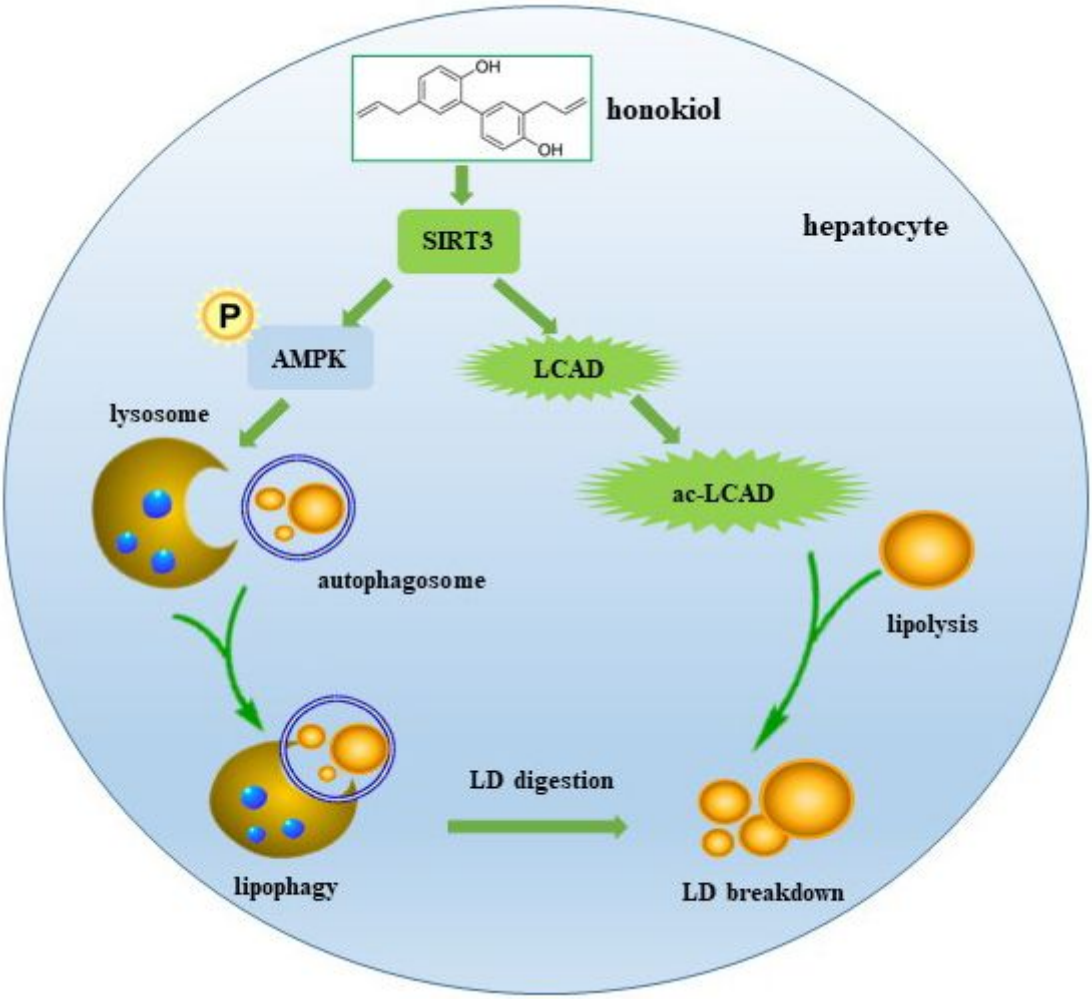

Figure 5

Schematic of the role of HK in protecting hepatocytes against lipotoxicity. HK activates SIRT3, which in turn activates AMPK to enhance autophagy on LDs and deacetylates LCAD to increase fatty acid oxidation in mitochondria, resulting in attenuation of lipotoxicity in hepatocytes.